www.sciencemag.org/cgi/content/full/1150841/DC1

Supporting Online Material for

Time-Resolved Observation and Control of Superexchange Interactions with Ultracold Atoms in Optical Lattices

S. Trotzky, P. Cheinet, S. Fölling, M. Feld, U. Schnorrberger, A. M. Rey, A. Polkovnikov, E. A. Demler, M. D. Lukin, I. Bloch*

*To whom correspondence should be addressed. E-mail: bloch@uni-mainz.de

Published 20 December 2007 on *Science* Express
DOI: 10.1126/science.1150841

This PDF file includes:

Supporting Online Material for:

Time-resolved Observation and Control of Superexchange Interactions with Ultracold Atoms in Optical Lattices

S. Trotzky,[1†] P. Cheinet,[1†] S. Fölling,[1] M. Feld,[1,2]
U. Schnorrberger,[1] A. M. Rey,[3] A. Polkovnikov,[4] E. A. Demler,[3,5]
M. D. Lukin,[3,5] and I. Bloch[1*]

[1]Institut für Physik, Johannes Gutenberg-Universität, 55099 Mainz, Germany
[2]Fachbereich Physik, Technische Universität Kaiserslautern, 67663 Kaiserslautern, Germany
[3]Institute for Theoretical Atomic, Molecular and Optical Physics,
Harvard-Smithsonian Center of Astrophysics, Cambridge, MA, 02138, USA
[4]Department of Physics, Boston University, Boston, MA, 02215, USA
[5]Physics Department, Harvard University, Cambridge, MA, 02138, USA

[*]To whom correspondence should be addressed; E-mail: bloch@uni-mainz.de.
[†]These authors contributed equally to this work.

Extended two-site Bose-Hubbard model. The inclusion of next-neighbor interactions to the simple BHM Hamiltonian defined in Eq. 1 leads to the extended two-site Bose-Hubbard Hamiltonian (*S1*)

$$\begin{aligned}\hat{H}^{\mathrm{EBHM}} &= \hat{H}^{\mathrm{BHM}} - \Delta J \sum_{\sigma\neq\sigma'} \left(\hat{n}_{\sigma\mathrm{L}} + \hat{n}_{\sigma\mathrm{R}}\right)\left(\hat{a}^\dagger_{\sigma'\mathrm{L}}\hat{a}_{\sigma'\mathrm{R}} + \hat{a}^\dagger_{\sigma'\mathrm{R}}\hat{a}_{\sigma'\mathrm{L}}\right) \\ &+ U_{\mathrm{LR}} \sum_{\sigma\neq\sigma'} \Big(\hat{n}_{\sigma\mathrm{L}}\hat{n}_{\sigma'\mathrm{R}} + \hat{a}^\dagger_{\sigma\mathrm{L}}\hat{a}^\dagger_{\sigma'\mathrm{R}}\hat{a}_{\sigma'\mathrm{L}}\hat{a}_{\sigma\mathrm{R}} \\ &\qquad + \frac{1}{2}\hat{a}^\dagger_{\sigma\mathrm{L}}\hat{a}^\dagger_{\sigma'\mathrm{L}}\hat{a}_{\sigma'\mathrm{R}}\hat{a}_{\sigma\mathrm{R}} + \frac{1}{2}\hat{a}^\dagger_{\sigma\mathrm{R}}\hat{a}^\dagger_{\sigma'\mathrm{R}}\hat{a}_{\sigma'\mathrm{L}}\hat{a}_{\sigma\mathrm{L}}\Big)\,, \end{aligned} \tag{S1}$$

where the parameters ΔJ and U_{LR} are defined in the main text. Here, we focus on a system of two coupled wells occupied by exactly two atoms in the two different spin-states $|\uparrow\rangle$ and $|\downarrow\rangle$. The relation of ΔJ and U_{LR} to the tunneling matrix element J is plotted in Fig. S1. It is apparent that those terms in Eq. S1 proportional to ΔJ act in the same way on an arbitrary Fock state in the system as the tunneling operator does and therefore modify J to now $J' = J + \Delta J$, while the terms proportional to U_{LR} lead to an energy shift of the states with exactly one atom on each site with respect to the states with double occupancy in a single well. The states $|s\rangle$ and $|-\rangle$ stay eigenstates of the system and the states $|t\rangle$ and $|+\rangle$ are now coupled via the matrix

$$H_{t,+}^{\mathrm{EBHM}} = \begin{pmatrix} 2U_{\mathrm{LR}} & -2J' \\ -2J' & U + U_{\mathrm{LR}} \end{pmatrix} \tag{S2}$$

with the eigenvalues

$$\pm\hbar\omega_{1,2}^{\mathrm{EBHM}} = \frac{U - U_{\mathrm{LR}}}{2}\left(1 \pm \sqrt{\left(\frac{4J'}{U - U_{\mathrm{LR}}}\right)^2 + 1}\right) + 2U_{\mathrm{LR}}\,, \tag{S3}$$

which correspond to the Fourier components for the evolution of the initial state $|\uparrow,\downarrow\rangle$ under the Hamiltonian Eq. S1. In the regime of strong interactions, the frequency ω_2 is assigned to the superexchange process and by means of perturbation theory up to second order one finds the effective coupling parameter to be $J'_{\mathrm{ex}} = 2J'^2/U - U_{\mathrm{LR}}$. The direct spin-exchange term U_{LR} favors an antiferromagnetic ground state for repulsively interacting bosons. However, the inset in Fig. S1 shows, that the case $U_{\mathrm{LR}} > 2J'^2/U$ is never reached and therefore the presence of the direct nearest neighbor interactions does not lead to a violation of the Lieb-Mattis theorem (*S2*). With $V_{\mathrm{long}} = 10E_r$ and $V_{\mathrm{trans}} = 41E_r$, the dependency of the two contributions on the short-lattice depth is well approximated by two exponential laws of the type $B_{\mathrm{s,d}} \times \exp(-\frac{1}{2}V_{\mathrm{short}}/E_r)$, where $B_{\mathrm{s}} = 15.24E_r$ for the superexchange term and $B_{\mathrm{d}} = 0.36E_r$ for the direct exchange term.

Loading sequence. Since the short lattice is created by a Gaussian laser beam at a wavelength of $765\,\mathrm{nm}$, it is blue-detuned with respect to the rubidium D1 and D2 transition and thus creates

an anti-confining potential in transversal direction. The simultaneous ramp up of the short lattice ($\sim 25\, E_r$) together with the red-detuned transversal lattices ($840\,\mathrm{nm}$ laser wavelength, $\sim 41\, E_r$) leads to a spreading of the atom distribution before freezing out tunneling and therefore to a more homogeneous filling than would be obtained by a fully red-detuned 3D optical lattice with the same beam waist and atom number. Subsequently, the long lattice is ramped up to $\sim 10\, E_r$ to obtain isolated double wells. The lattice depths during the loading and the shape of the ramps have been optimized to give mean occupation of each double well sites close to two. By means of an interferometric measurement similar to the one described in (*S3*), we verify that about 70-80% of the atoms are loaded to doubly occupied sites which is compatible with the conversion efficiency we observe in the spin-changing collisions.

Detection and filtering sequence. For each double well, we transfer the population of the left well into the second excited band of the underlying long lattice well by applying a tilt and ramping down the barrier afterwards (*S3, S4*). A subsequent adiabatic band mapping (*S5, S6*) results in spatial separation of the atoms initially localized on either side of the double well after TOF. A Stern-Gerlach filter at the beginning of TOF allows for a spin-state selective detection. In addition, we transfer those atoms that have not undergone the spin-changing collisions and therefore stayed in $|F = 1, m_F = 0\rangle$ with a microwave π-pulse to $|F = 2, m_F = 0\rangle$. They are removed by a resonant laser pulse during time-of-flight expansion to obtain the signal only from atoms in doubly occupied sites.

Since the wave functions of both atoms are brought to overlap during the detection sequence, a direct exchange term emerges which leads to spin-oscillations between the atoms initially located on separate sites (*S7*). To minimize this effect, we carry out the band mapping immediately ($\simeq 70\,\mu\mathrm{s}$) after the transfer. Since we cannot suppress the direct spin-exchange oscillations completely in our sequence, we believe these to limit our detection efficiency, while

the fidelity of the preparation is probably higher and therefore closer to the expected 99%.

Validity of the extended two-site Bose-Hubbard model. We investigate the validity of the EBHM by means of the frequency difference $\omega_1 - \omega_2$ in Fig. S2. While for low barrier depth, the EBHM models the data much better than the simple BHM, we still find deviations from its predictions which exceed the 2% uncertainty in our lattice depth. One reason for this can be the fact that the parameters for the BHM as well as for the EBHM are obtained by a single particle band structure calculation which does not account for the atom-atom interaction in the pairs. For a repulsive interaction and atom numbers larger than 1, a broadening of the single particle wave function has to be taken into account, which leads to lower onsite and higher intersite interaction energies (*S8, S9*). The comparison of the measurements to the solution of the two-band Schrödinger equation which includes the interaction from the start already shows a much better agreement. When more bands are taken into account, the two-frequency approximation used to fit the data is not valid anymore a direct comparison to the fit results is therefore not reasonable.

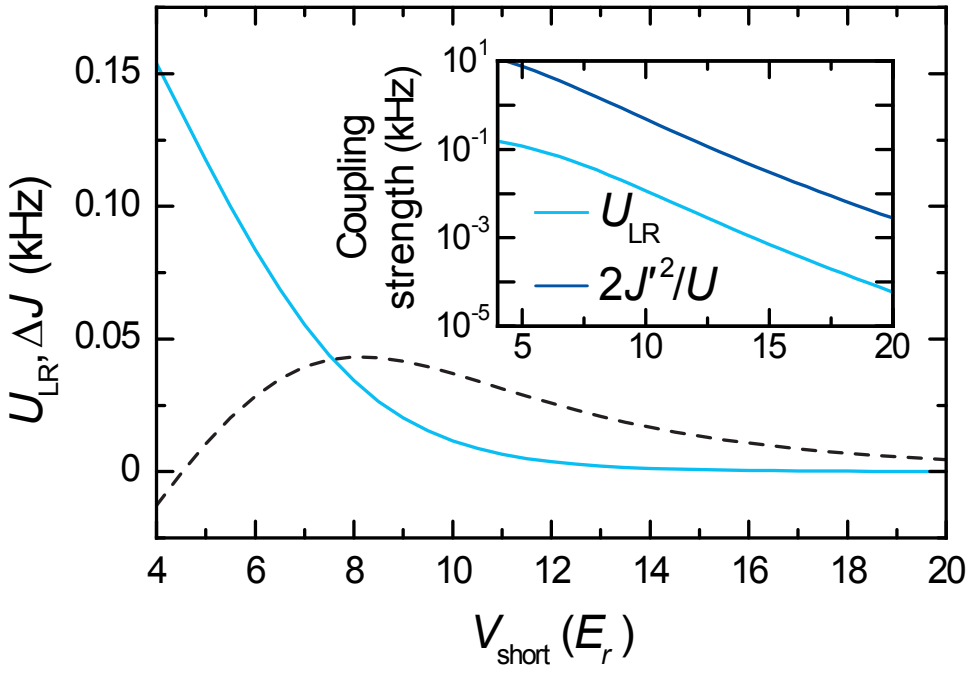

Figure S1: Extended Bose-Hubbard parameters. The parameters U_{LR} (light blue curve) and ΔJ (black dashed curve) are plotted versus V_{short}. The inset shows a comparison of the direct exchange term U_{LR} (light blue) to the superexchange term $2J'^2/U$ (dark blue), where the latter is always at least one order of magnitude larger than the first.

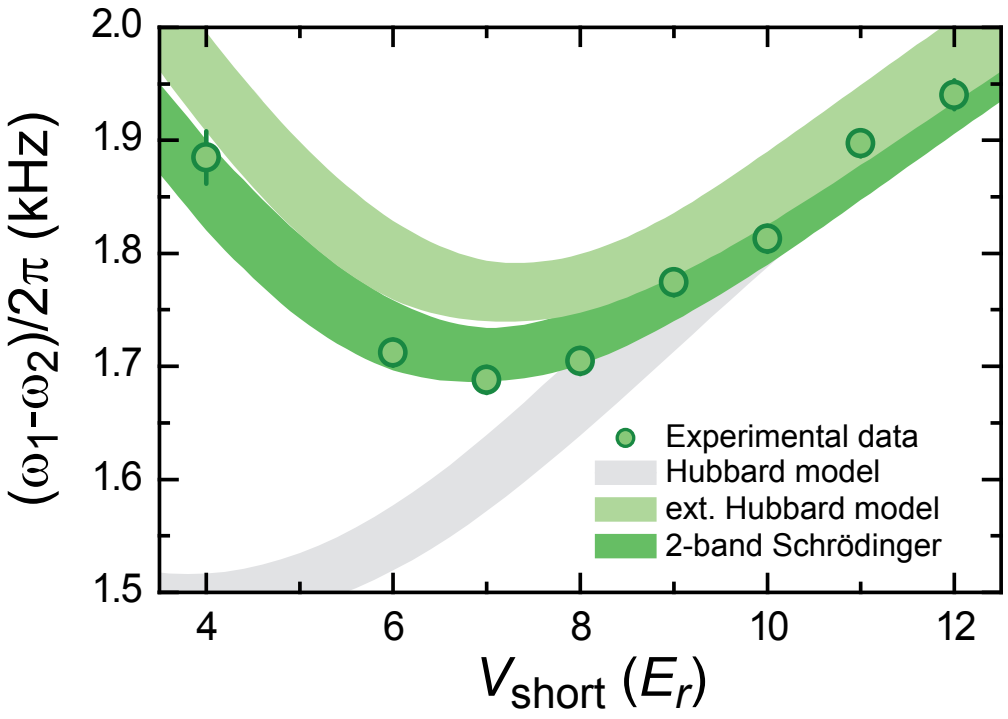

Figure S2: Comparison of the different models. The difference of the fitted frequencies $\omega_{1,2}/(2\pi)$ versus V_{short} are plotted as in Fig. 4A and compared to the predictions of the simple BHM (grey region, U/h), the EBHM (light green region, $(U + 3U_{\mathrm{LR}})/h$) and the solution of the two-band Schrödinger equation (dark green region). The width of the regions reflects the 2% uncertainty in lattice depths and the error bars on the data points denote the 95% confidence interval as obtained from the fits.

References and Notes

S1. V. Scarola, S. D. Sarma, *Phys. Rev. Lett.* **95**, 033003 (2005).

S2. E. Lieb, D. Mattis, *Phys. Rev.* **125**, 164 (1962).

S3. J. Sebby-Strabley, *et al.*, *Phys. Rev. Lett.* **98**, 200405 (2007).

S4. S. Fölling, *et al.*, *Nature* **448**, 1029 (2007).

S5. A. Kastberg, W. D. Phillips, S. L. Rolston, R. J. C. Spreeuw, P. S. Jessen, *Phys. Rev. Lett.* **74**, 1542 (1995).

S6. M. Greiner, I. Bloch, M. O. Mandel, T. Hänsch, T. Esslinger, *Phys. Rev. Lett.* **87**, 160405 (2001).

S7. M. Anderlini, *et al.*, *Nature* **448**, 452 (2007).

S8. G. Campbell, *et al.*, *Science* **313**, 5787 (2006).

S9. J. Li, Y. Yu, A. M. Dudarev, Q. Niu, *New J. Phys.* **8**, 154 (2006).